# Science and practice of imaging physics through 50 years of SPIE Medical Imaging conferences

Adam Wang,[a,*] Ian Cunningham,[b] Mats Danielsson,[c] Rebecca Fahrig,[d,e]
Thomas Flohr,[d] Christoph Hoeschen,[f] Frederic Noo,[g] John M. Sabol,[h]
Jeffrey H. Siewerdsen,[i] Anders Tingberg,[j] John Yorkston,[k]
Wei Zhao,[l] and Ehsan Samei[m]

[a]Stanford University, Department of Radiology, Stanford, California, United States
[b]Western University, Robarts Research Institute, London, Ontario, Canada
[c]KTH Royal Institute of Technology, Department of Physics, Stockholm, Sweden
[d]Siemens Healthineers, Forchheim, Germany
[e]Friedrich-Alexander Universität, Department of Computer Science, Erlangen, Germany
[f]Otto-von-Guericke University, Institute of Medical Engineering, Magdeburg, Germany
[g]University of Utah, Department of Radiology and Imaging Sciences, Salt Lake City, Utah, United States
[h]Konica Minolta Healthcare Americas, Wayne, New Jersey, United States
[i]Johns Hopkins University, Department of Biomedical Engineering, Baltimore, Maryland, United States
[j]Lund University, Skåne University Hospital, Department of Translational Medicine, Medical Radiation Physics, Malmö, Sweden
[k]Carestream Health, Rochester, New York, United States
[l]Stony Brook University, Department of Radiology, Stony Brook, New York, United States
[m]Duke University, Department of Radiology, Durham, North Carolina, United States

## Abstract

**Purpose**: For 50 years now, SPIE Medical Imaging (MI) conferences have been the premier forum for disseminating and sharing new ideas, technologies, and concepts on the physics of MI.

**Approach**: Our overarching objective is to demonstrate and highlight the major trajectories of imaging physics and how they are informed by the community and science present and presented at SPIE MI conferences from its inception to now.

**Results**: These contributions range from the development of image science, image quality metrology, and image reconstruction to digital x-ray detectors that have revolutionized MI modalities including radiography, mammography, fluoroscopy, tomosynthesis, and computed tomography (CT). Recent advances in detector technology such as photon-counting detectors continue to enable new capabilities in MI.

**Conclusion**: As we celebrate the past 50 years, we are also excited about what the next 50 years of SPIE MI will bring to the physics of MI.

## 1 Introduction

Since the first SPIE meeting on medical imaging (MI) in 1971, the conference has played an integral role in the development of countless technologies for MI. That first conference (*Quantitative Imagery in the Biomedical Sciences I*) covered a range of physics-related topics,

---

*Address all correspondence to Adam Wang, adamwang@stanford.edu

**Table 1** Major subfields of imaging physics discussed in this paper.

| Subfield |
| --- |
| Image science |
| Image quality metrology |
| Radiography |
| FPDs |
| Mammography |
| Fluoroscopy |
| Tomosynthesis |
| Cone-beam CT |
| Image reconstruction |
| Diagnostic CT |
| PCDs |

including image quality, image perception, and radiography. In the decade after, physics continued to play a central role in SPIE meetings of MI until the word "physics" first appeared in a conference title in 1982 (*Physics and Engineering in Medical Imaging*). Throughout the 1980s, annual meetings on MI topics continued to include physics through instrumentation, image formation, image processing, image quality, and more. MI became a regular, annual conference in 1987 and quickly expanded to multiple subconferences, where *Physics of Medical Imaging* became a mainstay since 1993. The conference has been largely informed by proffered papers, reflecting the progression of the field and serving as the premier venue for researchers and scientists to present and discuss important new developments.

The physics topics served MI technology and practice, with progression across modalities, metrologies, technologies, and applications. For example, the early days of linear systems theory described the transfer of imaging information through an analog screen-film x-ray system. These concepts were then applied to the new flat-panel digital detectors that dramatically changed the face of diagnostic radiology in the 1990s. More recently, the introduction of neural networks holds the promise of a similar sea change in the delivery of patient care. SPIE has always been the event where the field has congregated to see the future.

The purpose of this paper is to demonstrate and highlight the major trajectories of imaging physics and how they are informed by the community and science presented (largely but not exclusively) at SPIE MI conferences from its inception to now. In a broad stroke, we identify the field development through SPIE into 11 subfields detailed below (Table 1), which interrelate with each other in many ways. This list is by no means comprehensive, but rather reflective of the progression of the discipline as witnessed and highlighted through SPIE MI. As a result, many categories, modalities, and topics will not be covered due to limited focus and space. In addition, we aim to highlight a representative sample of SPIE MI papers showing the breadth of topics presented at SPIE conferences, but these are only a small sample of the many outstanding papers presented over the years and even then are not chosen to single out the "best" ones. Using the titles of the top five downloaded abstracts from each year, we generated a word cloud that represents the most common words (Fig. 1). As can be seen, these represent many familiar topics including imaging, x-ray, detector, digital, image, radiography, mammography, noise, and more. They highlight many concepts that together form the scaffolding of what we recognize as the physics of medical imaging.

**Fig. 1** Word cloud of most frequent words in *SPIE Physics of Medical Imaging* paper titles.

## 2 Image Science

About 50 years ago, scientists met at the SPIE MI conference to present and discuss new discoveries in image science that represented the start of a knowledge revolution with profound implications for medical care. This exciting field has moved from the maturing of film-based technologies and early discoveries in electronic imaging, through the discovery of physical principles that determine the performance and image quality of new technologies, to recent advances in photon counting technologies, noise reduction methods, and the use of artificial intelligence (AI) for image reconstruction and interpretation. This section highlights some of these key contributions to image science.

In the early 1970s, x-ray image intensifiers (XRII) were used with optical beam splitters to capture moving images both on 35-mm film and analog charge-coupled device (CCD) cameras, and research was starting on quantitative methods to characterize system performance. Early ideas on contrast ratio and modulation transfer function (MTF),[1] focal spot,[2] and x-ray spectral shape[3] were all introduced at SPIE meetings where scientists from the food and drug administration (FDA) were leading the push to develop quantitative metrics for quality assurance in these new technologies. While Fourier ideas were introduced in the 1950s,[4] practical use of MTF was still a novelty. At the 1979 SPIE meeting, Macovski[5] introduced the idea of dual-energy imaging and Ovitt et al.[6] introduced digital subtraction angiography (DSA) including a section on the benefits of using a digital image format. Thus started the digital revolution in image science.

Image science became a serious topic in the 1980s. Particular contributions came from Wagner, Burgess, Shaw, Barrett, Myers, and colleagues including the use of statistical decision theory and signal-to-noise ratio (SNR) concepts. For example, at the 1981 SPIE meeting, Wagner et al.[7] and Tapiovaara and Wagner[8] described the importance of the squared-SNR in detection theory and concepts of information transfer efficiency (Fig. 2). These led to widespread



**Fig. 2** X-ray tube voltage dependence of some radiographic task-dependent DQEs. The curves correspond to 20-cm phantom thickness and are for detecting a small thickness of target material. Reprinted from Ref. 8.

use of the detective quantum efficiency (DQE) including the noise-equivalent quanta (NEQ).[9] At the 1984 SPIE meeting they described a generalized DQE approach that described energy-dependent weights that would improve iodine SNR, something that would not be possible until the development of photon-counting detectors (PCD).[8] A series of articles and presentations introduced human signal-detection theory to radiographic imaging with the common feature that detection tasks in radiographic images are often noise limited.[10] Much of this work is summarized in an International Commission on Radiation Units & Measurements (ICRU) report including the importance of Fourier methods and connection to detectability index and ideal observers in 1996.[11] The idea that quantum-based imaging systems could be represented as a cascade of simple gain and blur processes was introduced.[12,13] Barrett led the development of digital spatial-domain methods to study detectability and system performance that is more comprehensive and appropriate for digital imaging systems.[14–16]

The 1990s and 2000s saw widespread adoption of Fourier and spatial-domain metrics for the description of the image signal and noise,[17,18] including developments in cascaded-systems theory which started in the 1980s to describe the connection between system design and performance metrics.[19,20] The use of Fourier metrics continues to this day, with the modern iterative and nonlinear image processing and noise reduction algorithms necessitating assessment conditions that are needed to satisfy the linearity and shift-invariance requirement of Fourier methods.[21] New concepts in image science are required to keep pace with the growth of AI to provide the scientific basis of these methods and provide an understanding of their potential to improve detection tasks and optimize image quality.

## 3 Image Quality Metrology

Concepts for measuring image quality are intimately tied to developments in image science. At the beginning of the 1970s most of the imaging systems broadly used were still two-dimensional (2D) and based on analog imaging detector configurations, e.g., based on screen-film systems or image intensifier tubes. These were tested regarding their image quality by using Fourier-based metrics such as MTF and DQE, but also low-frequency contrast tests, field evaluation, focus determination, and easy contrast tests as, e.g., presented in 1974.[1] Shaw and van Metter developed a theoretical approach for MTF and DQE measurements of screen-film systems in 1984[22] while together with Bunch, they looked into signal-to-noise measurements of such systems,[23] which was in a way following the descriptions by Wagner and Weaver in 1974.[24] Wagner and Brown[25] presented in 1984 a "more unified analysis of medical system SNR characteristics" (Fig. 3), representing the NEQ of three different screen-film-systems. The approach presented in this paper derived the ideal observer SNR based on statistical decision theory, which linked measurable values to the decision required in radiological imaging. This approach was further followed and investigated.[15] The link between physics-based measurements and the task of detection was established more clearly in the following years.[16] In parallel, studies describing the human observer performance on MI systems were conducted.

Beginning with the broader implementation of CT systems as well as digital imaging detectors for radiography and fluoroscopy, there were new lines of image quality assessment for such systems either based on Fourier-based or spatial-based approaches, both having advantages and disadvantages. It became clear, that the limitations of the digital systems had to be understood and that the image output might depend on the information content to be detected. Thus, papers were looking for the information content of the information patterns.[26] To keep pace with the fast development of new types of imaging systems, methods were developed to more practically assess achievable image quality and the ability to provide an estimate of the detectability of lesions or pathology using such imaging systems. An example study evaluated the generalized NEQ and a detectability index for tomosynthesis and cone-beam CT.[27] In addition, efforts are being made to measure the image quality or relevant descriptors of it no longer on phantom images or for artificial tasks but in the patient images itself first introduced at SPIE.[28,29] This has also extended to 3D imaging like CT,[30–32] found to be directly relatable to diagnostic performance.[33] It can be hoped that by such approaches, closer links between diagnostic performance and the determined image quality can be gained in the future. This might lead to new
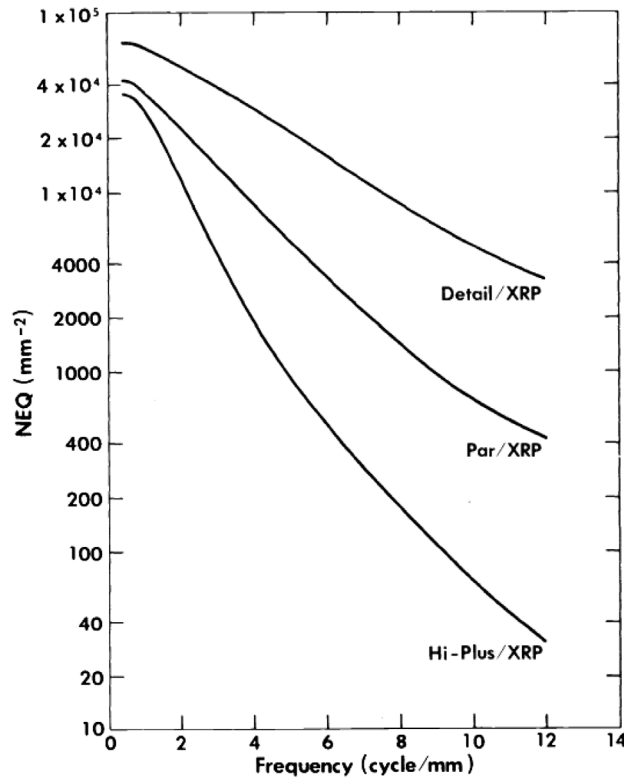
**Fig. 3** NEQ spectrum for three calcium tungstate screen/film systems at optical density = 1.0. Reprinted from Ref. 25.

concepts for optimization based on targeting acceptable image quality levels.[34] This is of great importance given the broad range of developments for new types of imaging systems and image reconstruction methods based on AI. Especially with respect to AI-based methods, new approaches for image quality assessment and quality assurance will be needed.

## 4 Radiography

Radiography is the oldest MI modality, and while its earlier developments predate SPIE, the Physics conference has provided many significant contributions. Because of its importance as a modality and relative simplicity in implementation, radiography has long been at the forefront of adopting new technologies and ideas. By 1980, the advantages of digital radiography (DR) were clear, including advantages in dose, scatter reduction, ease of operation, data transmission, image storage, flexible display capability, and image manipulation such as edge enhancement, filtering, and subtraction.[35] While analog radiology was still well entrenched and continued to be important,[36,37] DR extended the lessons learned from analog technologies to offer new advantages. The SPIE *Conference on Digital Radiography* in 1981 already recognized applications in DSA,[38] digital tomosynthesis,[39] and dual-energy radiography (Fig. 4).[40] Although the advantages of digital systems were described early on, improving their image quality and their acceptance in clinical practice still took considerable time and effort. For example, pixel size may be an obvious consideration for spatial resolution, but the effects of converter material and thickness, photodiode (PD) gain, and electronic noise all play an important role in image quality. Other considerations include field coverage, uniformity, quantum efficiency, sensitivity, dynamic range, acquisition speed, frame rate, noise characteristics, and cost. Initial DR systems were based on computed radiography (CR), which uses a photostimulable phosphor to capture and store the image, which is then read out with a laser system.[41,42] While CR has a large dynamic range, is digital and is portable, imaging plates must be processed through a reader and intrinsic image quality was seen as lacking.[43] Numerous other DR approaches were developed,[44] but the second generation of DR largely made use of flat-panel detectors (FPD) systems, which
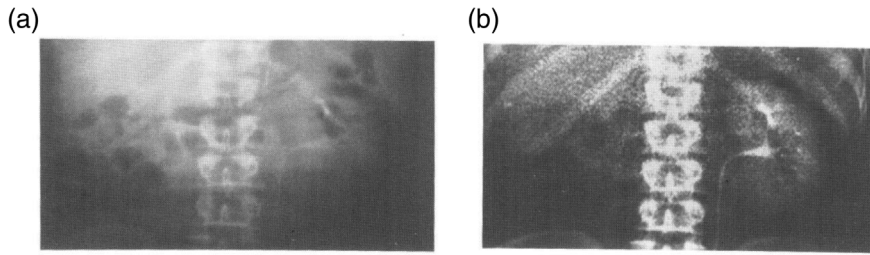
(a)    (b)



**Fig. 4** Digital pyelographic image (a) and corresponding dual-energy soft tissue subtraction view (b) for a patient with renal carcinoma. Reprinted from Ref. 40.

directly readout digital images. In addition to the instant readout, the advantages of FPDs in high efficiency and spatial resolution made them almost ideal for radiography.[45]

The developments in radiography were intertwined with developments in image science and detectors (described in those sections). Even today, radiography continues to evolve, with recent advances including dark-field chest radiography[46] and twin-robotic arms for flexible positioning and setup.[47]

## 5 Flat-Panel Detectors

The development of digital FPD (also referred to as flat-panel imagers) has been central to the development of many x-ray based modalities, including radiography, mammography, fluoroscopy, tomosynthesis, and cone-beam CT. The SPIE MI physics conference has always been the platform for presenting original ideas of the design, fabrication, and evaluation of FPD, with over 300 articles on this topic since 1991. With the breadth of knowledge in DR and imaging physics in the first two decades of SPIE MI, it was natural (in 1991) to hear the first presentation on the application of amorphous silicon (a-Si) PD in radiotherapy and diagnostic imaging, which was later referred to as the indirect FPD (Fig. 5).[48] The following year (1992) the first paper on amorphous selenium (a-Se) based, or direct conversion FPD was presented.[49] This decade saw a rapid growth of the number of SPIE presentations on both direct and indirect FPD, and an increasing number of contributions from the industry while FPD was being commercialized.[50–55] As FPD technology made its way through clinical translation, image quality evaluation and its standardization became an important topic of the conference.[56,57] Investigations presented at the conference became the foundation for International Electrotechnical Commission and other major standards for the evaluation of FPD.[58,59] Modeling techniques, such as the cascaded linear systems model, for FPD were extensively presented at the conference, and used to optimize FPD designs and identify potential areas of improvement.[60,61] It was realized that the low dose
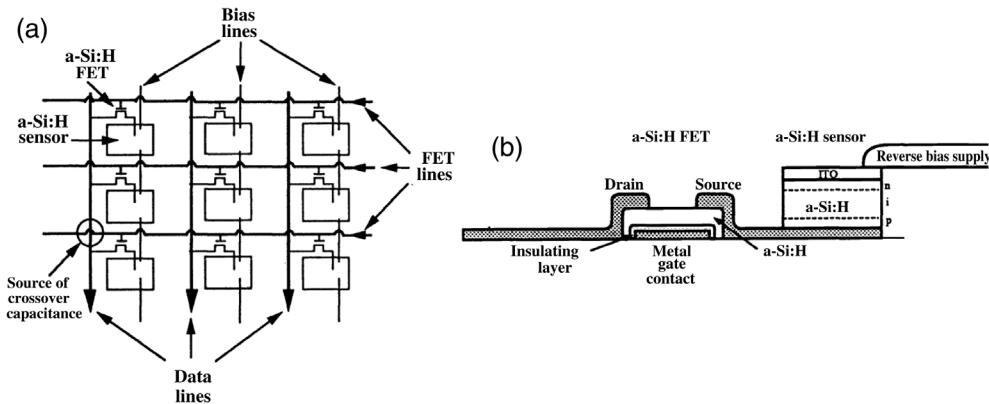


**Fig. 5** Schematic representation of a portion of a flat-panel imaging array. (a) Top view showing details of the PD sensors, field-effect transistors (FETs), and data, FET, and bias lines. (b) Cross-sectional view of sensor-FET combination for a single imaging pixel. Reprinted from Ref. 48.

performance of FPD is not x-ray quantum noise limited at the lowest exposures experienced in fluoroscopy. It became a major goal of the community to develop new FPD concepts and materials that could overcome this remaining issue of FPD.

Since 2000, many SPIE MI contributions have focused on novel ideas of how to improve the signal gain to overcome electronic noise in FPD. These ideas fall into two categories: (1) Decrease electronic noise by incorporating pixel amplification, referred to as active pixel sensor (APS); (2) Increase signal gain by using high conversion gain x-ray photoconductors, or optical detectors with avalanche gain. In the former category, pixel amplification was designed incorporating three transistors using either a-Si or polycrystalline Si (Poly-Si)[62,63] with prototype pixels or small arrays fabricated and tested. The lowest noise APS was achieved with crystalline silicon (c-Si) CMOS sensors. This was made possible with the advancement and cost-reduction in wafer-scale CMOS sensors, which were tiled to make FPD for medical x-ray imaging.[64–70]

To increase signal gain, avalanche amorphous selenium has been investigated for both direct and indirect detectors.[71,72] For x-ray quantum noise limited performance down to a single x-ray photon, a gain of 10 is sufficient.[73] For direct FPD, a variety of direct conversion materials were presented at the SPIE MI conference and drove industrial development for polycrystalline lead oxide (PbO), lead iodide ($PbI_2$), mercuric iodide ($HgI_2$), and cadmium telluride (CdTe).[74–77] More recently, organic–inorganic perovskite direct conversion FPD began to be presented at SPIE MI,[78] and we anticipate more work to be presented in future meetings, which will provide guidance for further development necessary for clinical translation and commercialization.

## 6 Mammography

The development of mammography over the last 50 years has been truly remarkable. National breast cancer screening programs have been introduced, which has had a huge impact on women's health, and the technical development has been extensive. In the early 1970s when the first SPIE MI symposium started, national breast cancer screening programs had not started yet; mammographic examinations were performed for diagnostic purposes. The first significant screening program was started in New York in 1963.[79] A decade later, screening trials were underway or had been carried out in a few different countries, e.g., USA, Sweden, and the UK.[80,81] From that point in time, national screening programs were implemented and became a strong driving force for new inventions in breast imaging. The development of the x-ray detector technology has been an important part of the SPIE MI symposia, together with other inventions in mammography.

X-ray mammography was originally carried out with nonscreen films, to achieve the high spatial resolution required for detecting calcifications. In the 1970s, dedicated screen-film systems for mammography were introduced with a 10 times reduction in dose.[81,82] Early attempts to convert the analog technique to digital included replacing the screen-film system with computed radiography[42,43] and slot-scan detectors.[83] Later the detector was replaced by FPDs, with a much faster read-out and significantly better DQE (Fig. 6).[64,84–86] Shortly after the FPDs were introduced, PCDs based on crystalline Si[87] or multichannel gaseous ionization chamber were invented.[88] Recently, a new generation of PCD based on GaAs was proposed.[89]

In parallel with the developments of new and improved mammography detectors, other techniques were invented to further increase the diagnostic performance of mammography and in particular screening. In the 1980s, automatic exposure control (AEC) systems and dedicated antiscatter grids for mammography were developed.[90] The AEC systems consisted originally of an ion chamber that controlled the exposure, whereas, in modern digital systems, the signal from the detector itself controls the exposure. The antiscatter grid prevents to a large extent the scattered radiation from reaching the detector, at the cost of an increased dose to the breast by a factor of 2.5 to 3. Recently, the virtual grids have shown promise to replace physical grids with the potential for reduced dose.[91]

As mammography became digital, new inventions became possible. Contrast-enhanced mammography,[92,93] digital breast tomosynthesis,[94–97] and contrast-enhanced breast tomosynthesis,[98,99] as well as breast CT,[100,101] have been invented. All these techniques have shown higher sensitivity and/or specificity than 2D digital mammography. Recently, mechanical imaging has also shown the potential to improve specificity.[102,103]
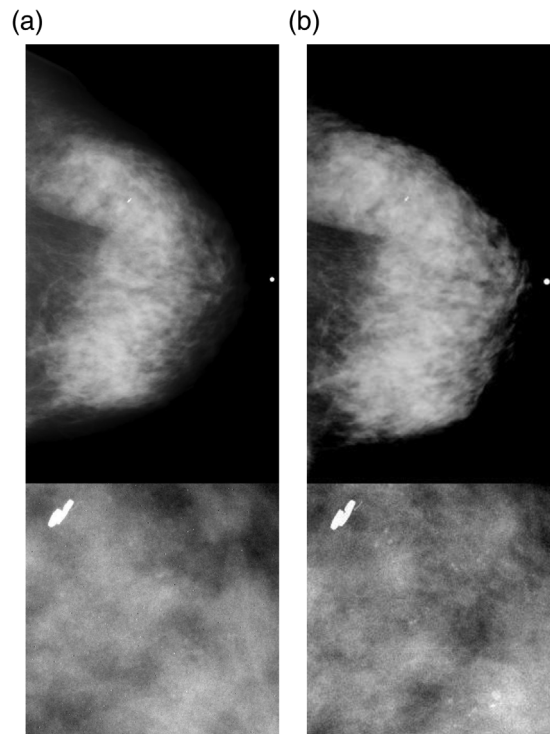
**Fig. 6** Clinical mammography images. The magnified inset is an enlargement of the biopsy marker. (a) Indirect conversion CsI + CCD (40-$\mu$m pixels). (b) Direct conversion selenium detector (70-$\mu$m pixels). Reprinted from Ref. 84.

## 7 Fluoroscopy

The advent of the XRII in the 1950s marked the adoption of x-ray fluoroscopic imaging and enabled the use of x-ray imaging during interventional and surgical procedures. An XRII consists of a cesium iodide phosphor deposited directly on the photocathode of an intensifier tube. Impinging x-ray photons create electrons that are accelerated and minified until hitting an output phosphor, producing an image ~105 times brighter than the input image. By capturing the ~2.5-cm diameter output image with a video camera, an interventionalist could visualize high-contrast devices and contrast-filled vessels in real-time on a TV screen. Some of the earliest work at the SPIE MI conference in the 1970s characterized the image performance of XRIIs.[1] At around the same time, analog-to-digital conversion was applied to the video camera output signal, permitting digital storage and manipulation of x-ray images. This capability led to the first major revolution in fluoroscopy, the invention of DSA.[104,105] Early images published in 1978 are shown in Fig. 7.[6] Through the 1980s, digital technology also enabled dual-energy subtraction for bone and soft-tissue removal,[5] and laid the foundation for automated image analysis such as blood-flow (contrast-flow) measurement, device detection, and motion and image-distortion correction. In the same timeframe, further improvements in image quality were achieved by replacing the video camera with solid-state detector technology (e.g., CCD cameras).[106]

The second major revolution in x-ray fluoroscopic imaging arrived with the replacement of the XRII by the digital FPD. The development of flat panel technology through the 1990s as described above, but it is interesting to note that the SPIE MI conference provided a forum where industry and academia discussed technology developments in an open and cooperative environment that is not often seen in scientific exchanges.[53] The transition to a fully digital, geometrically accurate, wide dynamic range, linear signal image acquisition system enabled several important applications for fluoroscopy systems. Quantitation became possible and a significant body of work correcting for detector nonidealities such as lag,[107] bright-burn, nonlinearity, and patient and detector internal scatter was developed. Multimodality integration—that is overlay of 3D information into a real-time 2D fluoroscopic image using rigid or nonrigid registration algorithms—also became a standard component of fluoroscopy-guided minimally invasive
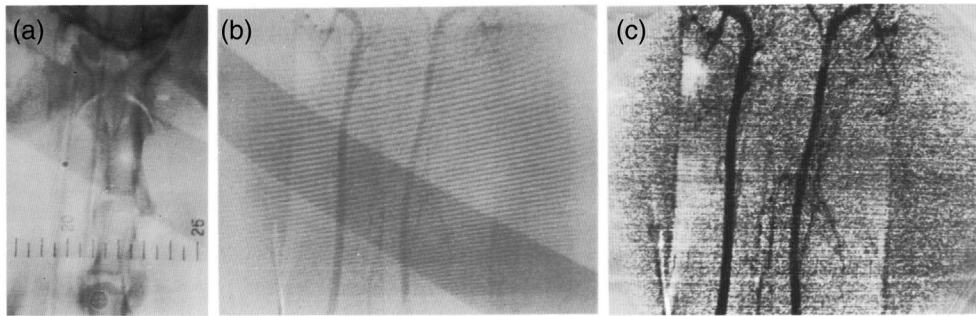
**Fig. 7** (a) Dog's neck with dilute contrast in the carotid arteries (not visible). (b) Subtracted image showing contrast. (c) Subtracted image with contrast stretching in the display. Reprinted from Ref. 6.

procedures, along with automatic device detection, device tracking, and device enhancement algorithms.[108,109] The basics of image quality and dose reduction in x-ray fluoroscopy will always be a focus at SPIE MI conferences; new technologies such as dynamic prepatient collimation, AI-based noise reduction, novel antiscatter grids, and more will continue to enable ever-more-complex minimally invasive image-guided interventions.

## 8 Tomosynthesis

About 50 years ago, at the time of the first SPIE MI meeting, tomographic imaging was only available through conventional tomography using film as the image detector. In the early 1970s, a number of investigators started to replace film with image intensifiers thus modifying these analog systems to enable digital capture and analysis. Baily and colleagues[110] described a fluoroplanigraphy system in 1971 with the potential for image digitization and subsequent image processing. A decade later, they described the realization of a digitized tomography system.[111] At the same time, CT scanners in projection (Scout view) mode were used to directly acquire digital radiographs that were used to synthesize arbitrary slice images.[39] It was not until the beginning of the new millennium that the development and readiness of flat panel digital detectors capable of rapid image read-out enabled viable tomosynthesis imaging systems to be the subject of widespread research and eventual clinical use. At this time, there was growth in system design and optimization research for musculoskeletal, thoracic, and mammographic applications. In addition, there was significant progress in the development of different reconstruction approaches. These included matrix inversion algorithms,[112] filtered back projection,[113,114] and iterative techniques.[94,115]

The initial impetus for tomosynthesis imaging was to improve thoracic imaging but this rapidly evolved to include musculoskeletal imaging applications[116] and the development of systems that could produce tomosynthesis images of all anatomies.[117] Radiographic tomosynthesis research has since progressed to rigorous clinical trials demonstrating efficacy[118] and continued efforts to apply new scientific and technical developments to enable novel clinical imaging applications including intraoral dental imaging[119] (Fig. 8) and real-time imaging in radiotherapy.[120]

Given the lack of an alternate tomographic imaging modality like CT, it is not surprising that the majority of tomosynthesis research and development has been focused on breast imaging. There continues to be considerable research into system design and optimization including pioneering work on tomosynthesis optimization at SPIE,[121] without a consensus on key factors such as optimal sweep angles, number of projections, and step-and-shoot versus continuous acquisition. These debates are likely to grow with increasing options resulting from the incorporation of new developments in x-ray sources, scanning geometries, reconstruction algorithms, and dose variation and reduction schemes. The need for the standard projection view in the exam and the generation and role of synthesized 2D views from the tomosynthesis data also continue to be investigated. As tomosynthesis has become the standard of care imaging technique for breast cancer screening, research and development efforts are turning from system design and validation to improving image quality, investigating novel imaging geometries and reconstruction
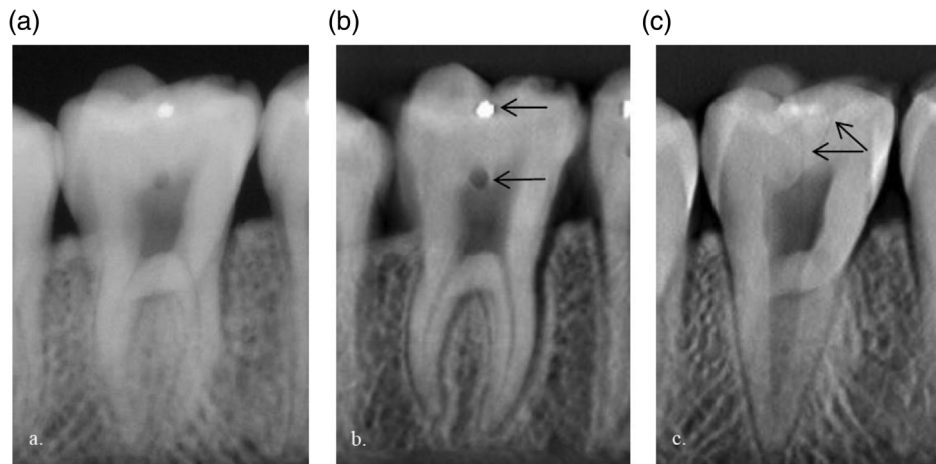
(a)          (b)          (c)



**Fig. 8** (a) 2D image of a tooth phantom containing a metallic filling, caries, and fractures. (b) Reconstructed tomosynthesis slice in the plane of the filling and the caries lesion. (c) Reconstructed tomosynthesis slice in the plane of the fractures. Note the increased detail in the lesions (arrows) and alveolar bone in (b) and (c). Reprinted from Ref. 119.

approaches, and developing tools and metrics for quality control including the development of dedicated phantoms for evaluating tomosynthesis systems.[122] Research trends include the expansion of tomosynthesis to include contrast-enhanced exams[123] and fusion with other imaging modalities, such as ultrasound.

Distributed x-ray sources provide unique imaging advantages and the opportunity for more flexible system design. Some of the earliest tomosynthesis research and development utilized a scanning-beam x-ray source in an inverse geometry in which the area of the source was much greater than that of the detector.[124] This system was designed for dynamic, real-time tomographic cardiac imaging. In the last decade, the application of distributed sources to tomosynthesis has become a growing area of research interest.[125] Undoubtably this trend will continue as distributed source array technology matures and becomes integrated into commercial systems. These source arrays enable greatly increased flexibility in system design and reduced acquisition times— ultimately enabling investigation of new or improved applications in breast and body imaging.

## 9 Cone Beam CT

Cone-beam computed tomography (CBCT) is among the important MI technologies for which SPIE MI has been an important forum in reporting early developments and clinical translation. Research at the turn of the century focused on the incorporation of FPDs in novel CBCT scanning systems and set the stage for systems to be developed in the following decades for a spectrum of diagnostic and interventional applications. Early work incorporated an FPD on a CT scanner gantry for possible application in 3D angiography.[126] CBCT was also developed for image-guided radiation therapy (IGRT),[127] which grew quickly to represent the standard of care in IGRT. That work was extended to mobile and fixed-room C-arms for CBCT in image-guided surgery and interventional radiology (Fig. 9).[128,129] Applications of CBCT in diagnostic imaging were soon to follow, including CBCT technologies for 3D breast imaging[130,131] as well as musculoskeletal imaging.[132]

CBCT image quality was an important topic throughout the development of such emerging systems to identify and mitigate the key factors that limited image quality, such as detector performance, x-ray scatter, and other sources of image noise and artifact. Such work drew from the foundations of MI physics, modeling of the imaging chain, and task-based imaging performance evaluation that were the hallmarks of the Physics of Medical Imaging conference throughout the 1980s (for screen-film systems) and the 1990s (for FPDs). Extending such models to CBCT, fully 3D NPS, NEQ, and task-based detectability index was applied to CBCT systems.[133] The role of x-ray scatter as a limiting factor in CBCT was well appreciated, and scatter artifact
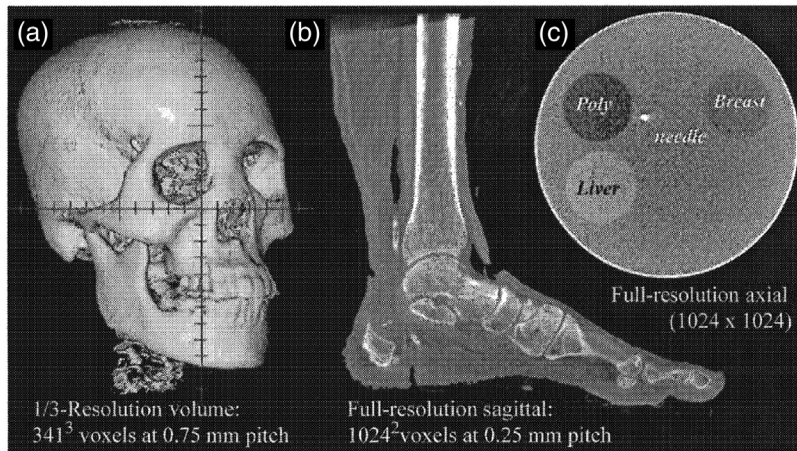
**Fig. 9** Various CBCT images: (a) surface rendering of skull phantom, (b) sagittal image of an amputated limb, and (c) transaxial image of a low-contrast phantom with a steel needle inserted in the field of view. Reprinted from Ref. 128.

correction methods ranged from parametric or Monte Carlo modeling[134] to beam-blocker and related methods.[135] As CBCT systems found prevalent clinical application in diagnostic and image-guided settings, ongoing work identified patient motion as an important aspect of image quality degradation, with a number of motion compensation methods under development.[136]

As CBCT systems found broad clinical application and their image quality limitations were fully appreciated, novel means of 3D image reconstruction formed an important area of research. Such work proceeded closely in step with similar activity in diagnostic helical CT, as described in greater detail below. Optimization-based alternatives to 3D filtered back projection were an active area of research, including model-based image reconstruction (MBIR) methods with improved noise-resolution tradeoffs. MBIR methods were demonstrated for CBCT,[137] including predictive models for imaging performance in MBIR[138] and extension to novel image acquisition protocols—e.g., noncircular orbits.[139] MBIR models were also extended to incorporate patient-specific prior information (e.g., from a previous CBCT scan) for CBCT applications in image-guided interventions.[140,141] Deep neural networks represent an important emerging basis for CBCT image reconstruction[142] raising important opportunities to improve image quality, to understand the fundamental limits to deep learning performance, and to better inform such approaches by the incorporation of physical models.

## 10 Image Reconstruction

Advances in image reconstruction have been critical to the development of diagnostic CT from a 2D parallel-beam imaging modality to the current fully 3D multidetector technology, as well as for the development of CBCT imaging for interventional radiology, oncology, and breast cancer screening and diagnostic. Presentations at the conference have closely followed and enabled these developments. To transition from parallel-beam CT to the current state-of-the-art CT technology, there once was the crucial need to discover how to perform a filtered back-projection reconstruction in the direct fan beam geometry when only a short scan of data is available. The problem was in the partial redundancy of the data, which appeared incompatible with the application of the ramp filter. Giving up on equal data weighting, in favor of utilizing a differentiable data weighting function,[143] was a major finding that not only supported the targeted application but enabled, through various extensions, the development of single-slice spiral (a.k.a. helical) CT in the early 1990s,[144,145] the expansion to multislice CT at the beginning of the century,[146] and the final transition to the fully 3D geometry of nowadays,[147–149] alongside with a simultaneous expansion of CT applications to include cardiac imaging.[150,151] While judicious data weighting schemes helped produce images of useful quality, it was understood early on that theoretically exact and stable reconstruction would require solving the fully 3D cone-beam
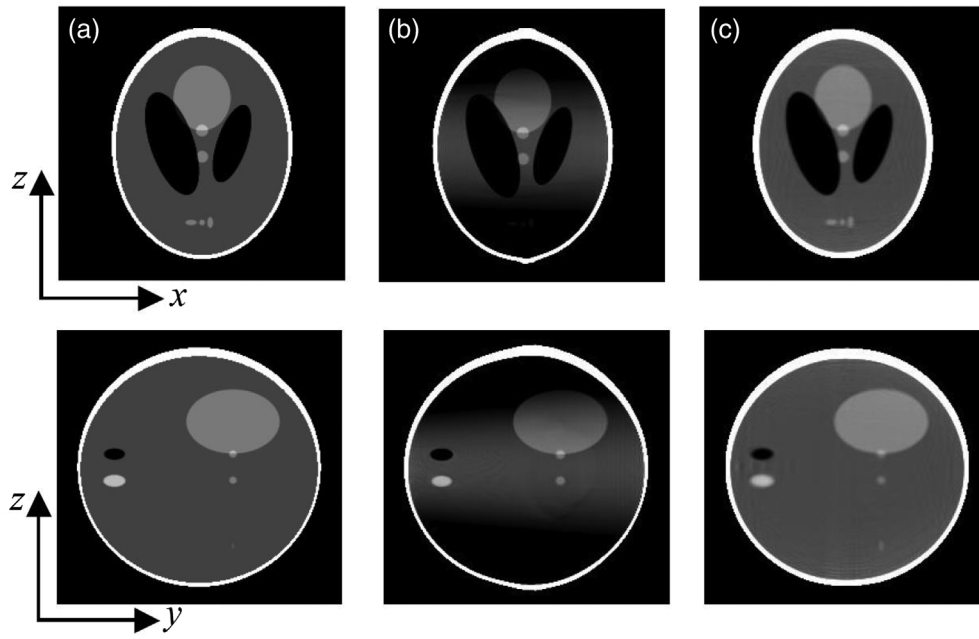
**Fig. 10** Different cone-beam CT reconstructions of simulated phantom. Top row: $xz$ plane, bottom row: $yz$ plane: (a) original phantom, (b) Feldkamp-type half-scan reconstruction, and (c) Grangeat-type half-scan reconstruction. Reprinted from Ref. 154.

image reconstruction problem.[152,153] This problem was extensively investigated for a circular trajectory (Fig. 10),[154–157] and the results have been beneficial for large cone angle diagnostic CT as well as cone beam imaging with FPDs. Down the road, amazing solutions emerged to handle axially truncated data as needed for multislice CT with a helical acquisition,[158,159] which played a major role in terms of algorithm refinements balancing cone-beam artifacts together with efficient use of radiation dose and mitigation of artifacts due to beam hardening and patient motion. Over time, great progress was also made for various other geometries,[160–164] which will support future advances in cone-beam CT with large area detectors.

Many applications of x-ray CT occur in a busy clinical environment, where fast workflow is a necessity. For this reason, image reconstruction scientists have also devoted important effort to the development of fast algorithms, by using more efficient mathematical reformulations,[165–168] or by identifying ways to benefit from novel computing hardware.[169–173] Such developments have been and remain critical as CT image reconstruction is evolving from linear to nonlinear methods, either with optimization techniques or deep learning paradigms or with a combination of these tools.[174–178] While optimization methods are still under investigation for CT, it is worth mentioning that they have been used for more than two decades in PET, due to the much smaller dataset size, with important advances then presented at the conference.[179–181] Last, we note that the conference served as an important venue to support image reconstruction developments in tomosynthesis for breast imaging, with contributions spanning dedicated analytical formulas,[114] optimization techniques,[182] and deep learning approaches.[183]

## 11 Diagnostic CT

Since its introduction in 1972, CT has advanced at a rapid pace and is now a pillar of radiological diagnosis. The first CT systems were mere head scanners, with an acquisition time of several minutes per image. In the 1980s whole-body CT scanners became available, with scan times per image reduced to a couple of seconds and significantly improved spatial resolution. However, only single axial slices of the patients' anatomy could be acquired. The ability of continuous rotation led to the development of spiral (helical) CT in the early nineties (Fig. 11)—this was a significant breakthrough in the history of CT.[144,184,185] For the first time, volume data became available without the risk of mis- or double-registration of anatomical details, albeit initially with
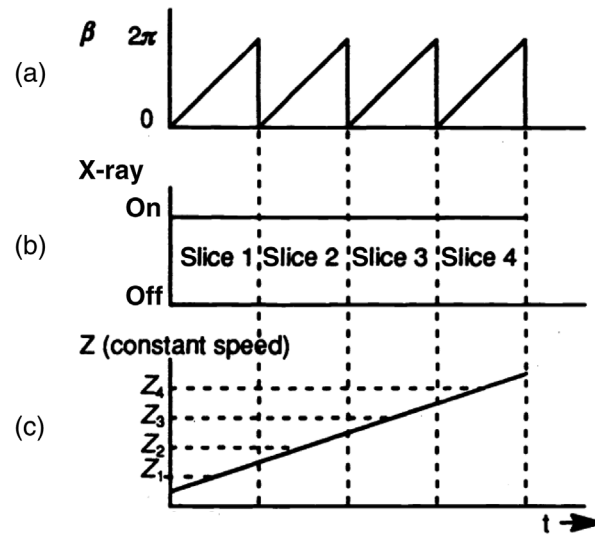
**Fig. 11** Schematic diagram for constant speed helical scanning (CSH), where $t$ indicates time. The gantry rotational angle $\beta$ is shown in (a) and the state of the x-ray source is shown in (b). The table location $z$ is shown for CSH in (c). Reprinted from Ref. 144.

limited scan ranges. Larger volume coverage in shorter scan times with thinner image slices was made possible by the widespread introduction of multidetector row computed tomography (MDCT) by all major CT manufacturers in 1998.[186,187] As a result of faster gantry rotation, MDCT also expanded into areas previously considered outside the scope of third-generation CT scanners, such as ECG-controlled cardiac imaging.[188] Interestingly, the basis for CT image reconstruction with optimized temporal resolution was already laid in the early 1980s.[143] The first decade of the 20th century was characterized by a race for more and more detector rows—4, 16, 32, 64-row scanners became available at a rapid pace. Consequently, new image reconstruction techniques came into focus that could cope with the increasing cone angles of the measurement rays.[189,190] Iterative reconstruction was investigated as a method to better account for the statistical properties of the CT data.[191]

Increasing clinical experience with MDCT indicated that adding even more detector rows alone would not result in greater clinical benefit. Instead, new CT concepts were evaluated to overcome the remaining limitations of MDCT. While several innovative CT designs never found their way into clinical routine,[192] two concepts held their own over the years: wide-area detector CT and dual-source CT. As a method of extending CT from purely morphologic to functional imaging, spectral CT imaging has experienced a renaissance. New reconstruction schemes[193] were proposed, techniques to acquire dual-energy CT data were evaluated,[194] and different ways to produce meaningful clinical results were investigated.[195–198] Most recently, another novel CT concept has gained increasing interest in the CT research community: photon-counting CT (described in greater detail below). The first results of photon counting CT systems with increasing maturity demonstrated potential clinical benefits (Fig. 12).[199–202] As the latest exciting development, machine learning has now also made its way into CT image reconstruction and is currently drawing a great deal of attention.[203,204]

## 12 Photon Counting Detectors

Photon counting is an intuitive way of detecting x-rays, counting them one by one, and measuring the energy for each x-ray using programmable thresholds. In nuclear imaging, such as single-photon emission computed tomography and PET, this has been the gold standard from the start. One advantage compared with energy integrating x-ray detectors is that electronic noise can be eliminated, enabling lower-dose imaging. The second advantage is that since the energy is measured for each x-ray, the information can be weighted to optimize the image quality when the image is formed. The energy measurement can also be used for improved separation between
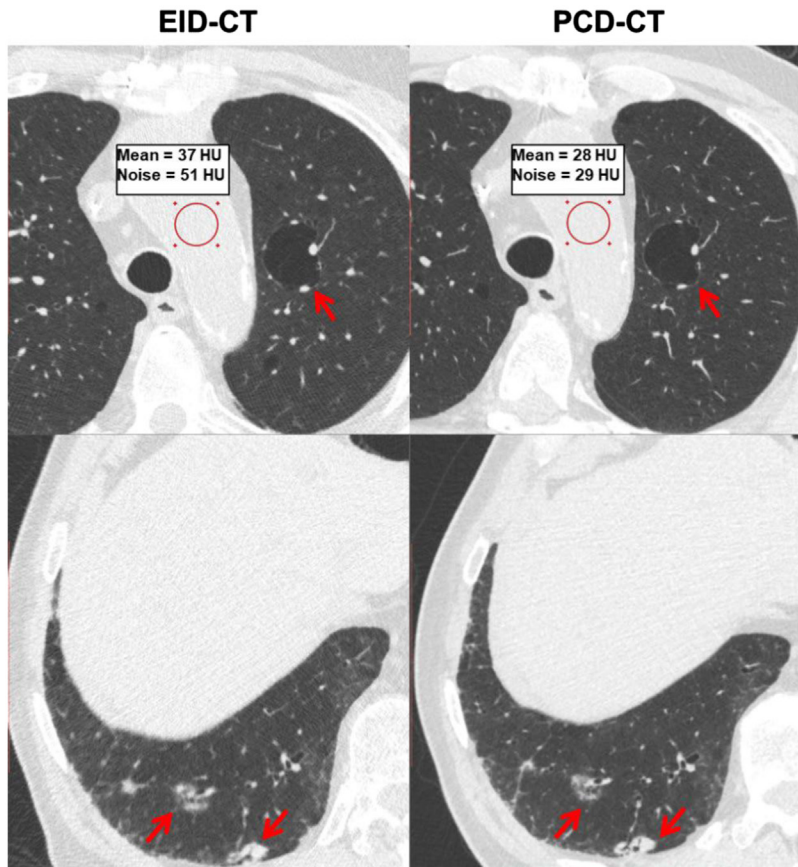
**Fig. 12** Chest patient images from conventional energy integrating detector (EID) CT and PCD CT comparing pathological features such as cystic air spaces (red arrows, upper row) and lung nodules (red arrows, bottom row). The conspicuity of anatomic details noticeably improved in PCD-CT images. The PCD-CT image also exhibited lower image noise than EID-CT at matched acquisition dose as shown in the ROI measurements. Reprinted from Ref. 199.

calcium and iodine, for example. Today's dual-energy solutions have significantly worse energy resolution and/or require unfavorable trade-offs in spatial resolution and workflow. PCDs are direct conversion with reduced pixel size, drastically increasing the spatial resolution. The first paper describing a PCD[87] that led to an FDA-cleared x-ray imaging system was presented at SPIE MI 2000 (Fig. 13). At that time, it was the only photon-counting paper at the conference. Since then, photon counting has grown into a major topic at the MI conference, and a large part of the progress in this field of research can be attributed to presentations and discussions in that forum.

One important area of progress has been on the hardware side with improved sensors and fast, low-noise application-specific integrated circuits.[201,205–207]

A major challenge with photon counting is the high incident rate of x-rays, and the following pile-up of events and charge sharing between pixels. Several contributions helped both to evaluate the impact on image quality and to suggest correction algorithms or detector design strategies to mitigate the problems.[208–212] Other noteworthy contributions investigated the potential for photon counting in terms of energy weighting and material basis decomposition.[213–216] Several promising clinical applications have been suggested, such as dual contrast imaging of the liver, kidney stones, and crystal-related arthropathies, cardiovascular imaging, thoracic imaging, and neuroradiology.[199,217–220] Two major technology platforms are currently being developed for photon-counting CT.[221] The first uses a cadmium-based (CdTe or CZT) sensor with a thickness of a few millimeters.[199] The second is based on so-called "deep silicon," with sensors being mounted in an edge-on geometry with several centimeters of depth. One system recently received FDA clearance, and we can expect regulatory clearance for several more systems
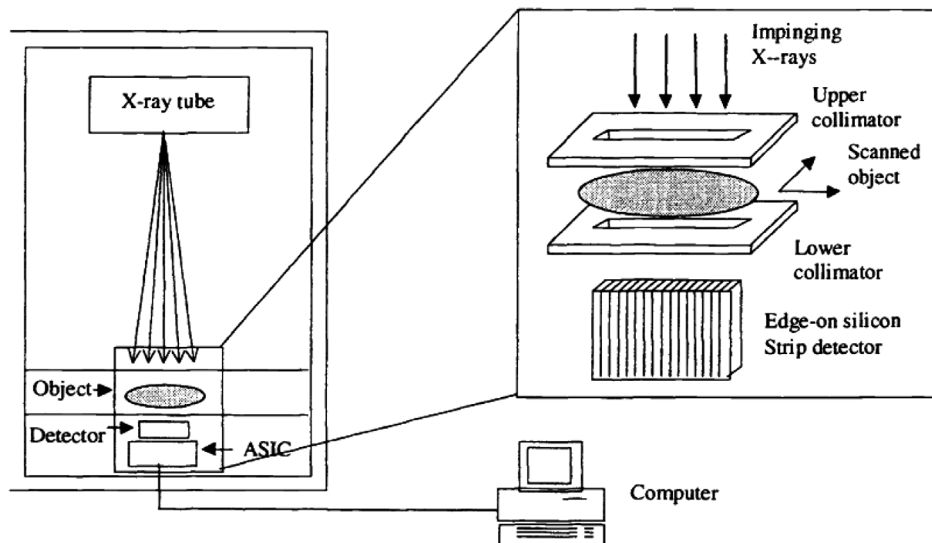
**Fig. 13** Dose-efficient x-ray system with edge-on silicon PCDs for digital mammography. Reprinted from Ref. 87.

in the next few years. Photon counting also paves the way for future clinical applications such as phase-contrast imaging. Ultrahigh spatial resolution down to 1 $\mu$m can be feasible,[222] and a pseudo-monochromatic beam can be achieved since the x-ray wavelength is measured.[223]

## 13 Conclusions

As these MI technologies developed from primitive concepts and prototypes to competing for commercial systems in routine use for many clinical applications, the SPIE MI meeting has served as an effective interface between the basic research of academic scientists, technology development of engineers, and the dissemination of industry research and development. The SPIE MI community played an instrumental role in many key developments in the past 50 years by sharing new ideas and results, learning from each other—ranging from experts in short courses to students giving talks and presenting posters, and forming lasting friendships and collaborations. That journey has never been simple. For today's community, it may be difficult to appreciate that the very concept of a "digital" MTF or DQE was controversial in the mid 1990s, yet today it is acknowledged as the methodology that accurately describes digital system performance and allows for system performance optimization. The recent discussions on neural networks, their configuration, the issues associated with their "learning/training," and the evaluation of their performance bear the same hallmarks of the birth of another game-changing technology. The SPIE MI conference will undoubtedly play a pivotal role in the development of this nascent field and many others that hold so much promise for the future betterment of patient care, and we are excited about what the next 50 years of SPIE MI will bring.

## Disclosures

## Acknowledgments

## References

1. M. P. Siedband, "How the user may specify and measure the performance of image intensifier systems," *Proc. SPIE* **0056**, 99–106 (1974).
2. K. E. Weaver, R. F. Wagner, and D. J. Goodenough, "Performance considerations of x-ray tube focal spots," *Proc. SPIE* **0056**, 150–158 (1974).
3. T. R. Fewell and K. E. Weaver, "The measurement of diagnostic x-ray spectra with a high purity Germanium spectrometer," *Proc. SPIE* **0056**, 9–18 (1974).
4. J. W. Coltman, "The specification of imaging properties by response to a sine wave input," *J. Opt. Soc. Am.* **44**(6), 468 (1954).
5. A. Macovski, "Iodine imaging using spectral analysis," *Proc. SPIE* **0167**, 67–76 (1979).
6. T. W. Ovitt et al., "The development of a digital video subtraction system for intravenous angiography," *Proc. SPIE* **0167**, 61–66 (1979).
7. R. F. Wagner, D. G. Brown, and C. E. Metz, "On the multiplex advantage of coded source/aperture photon imaging," *Proc. SPIE* **0314**, 72–76 (1981).
8. M. J. Tapiovaara and R. F. Wagner, "A generalized detective quantum efficiency (DQE) approach to the analysis of x-ray imaging," *Proc. SPIE* **0454**, 52–57 (1984).
9. R. M. Nishikawa and M. J. Yaffe, "Modelling of the spatial-frequency-dependent detective quantum efficiency of x-ray image receptors," *Proc. SPIE* **0914**, 128 (1988).
10. A. E. Burgess, R. F. Wagner, and R. J. Jennings, "Human signal detection performance for noisy medical images," *Proc. SPIE* **0372**, 99–105 (1982).
11. P. Sharp et al., "*ICRU report 54, Medical imaging—the assessment of image quality*," International Commission on Radiation Units and Measurements (1996).
12. P. L. Dillon et al., "Principles governing the transfer of signal modulation and photon noise by amplifying and scattering mechanisms," *Proc. SPIE* **0535**, 130 (1985).
13. M. Rabbani, R. Van Metter, and R. Shaw, "Detective quantum efficiency of imaging systems with amplifying and scattering mechanisms," *J. Opt. Soc. Am. A* **4**(5), 895 (1987).
14. H. H. Barrett et al., "Quantifying the performance of imaging systems," *Proc. SPIE* **0535**, 65 (1985).
15. K. J. Myers et al., "Is ideal-observer signal-to-noise ratio a good predictor of human performance?" *Proc. SPIE* **0535**, 12 (1985).
16. H. H. Barrett et al., "Detection and discrimination of known signals in inhomogeneous, random backgrounds," *Proc. SPIE* **1090**, 176 (1989).
17. C. E. Metz et al., "Toward consensus on quantitative assessment of medical imaging systems," *Med. Phys.* **22**(7), 1057–1061 (1995).
18. H. H. Barrett et al., "Generalized NEQ: Fourier analysis where you would least expect to find it," *Proc. SPIE* **2708**, 41–52 (1996).
19. I. A. Cunningham and R. Shaw, "Signal-to-noise optimization of medical imaging systems," *J. Opt. Soc. Am. A* **16**(3), 621 (1999).
20. J. Yao and I. A. Cunningham, "Parallel cascades: new ways to describe noise transfer in medical imaging systems," *Med. Phys.* **28**(10), 2020–2038 (2001).
21. M. Robins, J. B. Solomon, and E. Samei, "Can a 3D task transfer function accurately represent the signal transfer properties of low-contrast lesions in non-linear CT systems?" *Proc. SPIE* **10573**, 1057343 (2018).
22. R. Shaw and R. L. Van Metter, "An analysis of the fundamental limitations of screen-film systems for x-ray detection I. General theory," *Proc. SPIE* **0454**, 128–132 (1984).
23. P. C. Bunch, R. Shaw, and R. L. Van Metter, "Signal-to-noise measurements for a screen-film system," *Proc. SPIE* **0454**, 154–163 (1984).
24. R. F. Wagner and K. E. Weaver, "Noise measurements on rare-earth intensifying screen systems," *Proc. SPIE* **0056**, 198–207 (1974).

25. R. F. Wagner and D. G. Brown, "More unified analysis of medical imaging system SNR characteristics," *Proc. SPIE* **0454**, 2–8 (1984).
26. C. Hoeschen, E. Buhr, and W. Doehring, "High-spatial-resolution measurement of x-ray intensity pattern in a radiograph of the thorax," *Proc. SPIE* **3659**, 432–443 (1999).
27. G. J. Gang et al., "The generalized NEQ and detectability index for tomosynthesis and cone-beam CT: from cascaded systems analysis to human observers," *Proc. SPIE* **7622**, 76220Y (2010).
28. Y. Lin et al., "A patient image-based technique to assess the image quality of clinical chest radiographs," *Proc. SPIE* **7961**, 796160 (2011).
29. Y. Lin et al., "Quantification of radiographic image quality based on patient anatomical contrast-to-noise ratio: a preliminary study with chest images," *Proc. SPIE* **7627**, 76271F (2010).
30. J. Sanders, L. Hurwitz, and E. Samei, "Patient-specific quantification of image quality: an automated method for measuring spatial resolution in clinical CT images," *Med. Phys.* **43**(10), 5330–5338 (2016).
31. Z. Passand and C. Hoeschen, "Image quality assessment of real patient thorax CT images using modulation transfer function and noise power spectrum," *Proc. SPIE* **11312**, 113122N (2020).
32. O. Christianson et al., "Automated technique to measure noise in clinical CT examinations," *Am. J. Roentgenol.* **205**(1), W93–W99 (2015).
33. T. B. Smith, J. Solomon, and E. Samei, "In-vivo detectability index: development and validation of an automated methodology," *Proc. SPIE* **10132**, 1013255 (2017).
34. F. Ria et al., "Expanding the concept of diagnostic reference levels to noise and dose reference levels in CT," *Am. J. Roentgenol.* **213**(4), 889–894 (2019).
35. P. J. Bjorkholm, M. Annis, and E. E. Frederick, "Digital radiography," *Proc. SPIE* **0233**, 137–144 (1980).
36. P. C. Bunch, "Performance characteristics of high-MTF screen-film systems," *Proc. SPIE* **2163**, 14–35 (1994).
37. P. C. Bunch, "Comparison of high-MTF and reduced-noise radiographic imaging systems," *Proc. SPIE* **2432**, 67–95 (1995).
38. C. A. Mistretta, "Current practice and future directions in digital subtraction angiography," *Proc. SPIE* **0314**, 18–25 (1981).
39. D. G. Nishimura, A. Macovski, and W. R. Brody, "Digital tomosynthesis using a scanned projection radiographic system," *Proc. SPIE* **0314**, 31–36 (1981).
40. F. G. Sommer et al., "Abdominal dual energy imaging," *Proc. SPIE* **0314**, 172–174 (1981).
41. J. T. Dobbins et al., "DQE(f) of four generations of computed radiography acquisition devices," *Med. Phys.* **22**(10), 1581–1593 (1995).
42. S. Arakawa et al., "Improvement of image quality in CR mammography by detection of emissions from dual sides of an imaging plate," *Proc. SPIE* **3977**, 590–600 (2000).
43. J. A. Rowlands, "The physics of computed radiography," *Phys. Med. Biol.* **47**(23), R123–R166 (2002).
44. M. J. Yaffe and J. A. Rowlands, "X-ray detectors for digital radiography," *Phys. Med. Biol.* **42**(1), 1–39 (1997).
45. J. Rowlands and J. Yorkston, "Flat panel detectors for digital radiography," in *Handbook of Medical Imaging*, J. Beutel, H. L. Kundel, and R. L. Van Metter, Eds., Physics and Psychophysics, Vol. **1**, pp. 223–328, SPIE, Bellingham, Washington (2000).
46. P. B. Noel et al., "First experience with x-ray dark-field radiography for human chest imaging," *Proc. SPIE* **10132**, 1013215 (2017).
47. A. Fieselmann et al., "Twin robotic x-ray system for 2D radiographic and 3D cone-beam CT imaging," *Proc. SPIE* **9783**, 97830G (2016).
48. L. E. Antonuk et al., "Signal, noise, and readout considerations in the development of amorphous silicon photodiode arrays for radiotherapy and diagnostic x-ray imaging," *Proc. SPIE* **1443**, 108–119 (1991).
49. W. Zhao and J. A. Rowlands, "Large-area solid state detector for radiology using amorphous selenium," *Proc. SPIE* **1651**, 134–143 (1992).

50. D. L. Y. Lee, L. K. Cheung, and L. S. Jeromin, "New digital detector for projection radiography," *Proc. SPIE* **2432**, 237–249 (1995).

51. C. Chaussat et al., "New CsI/a-Si 17" x 17" x-ray flat-panel detector provides superior detectivity and immediate direct digital output for general radiography systems," *Proc. SPIE* **3336**, 45–56 (1998).

52. A. Tsukamoto et al., "Development of a selenium-based flat-panel detector for real-time radiography and fluoroscopy," *Proc. SPIE* **3336**, 388–395 (1998).

53. U. W. Schiebel et al., "Fluoroscopic x-ray imaging with amorphous silicon thin-film arrays," *Proc. SPIE* **2163**, 129–140 (1994).

54. J. Chabbal et al., "Amorphous silicon x-ray image sensor," *Proc. SPIE* **2708**, 499–510 (1996).

55. R. L. Weisfield et al., "Improved page-size 127-$\mu$m-pixel amorphous-silicon image sensor for x-ray diagnostic medical imaging applications," *Proc. SPIE* **3032**, 14–21 (1997).

56. E. Samei et al., "DQE of direct and indirect digital radiography systems," *Proc. SPIE* **4320** 189–197 (2001).

57. V. Loustauneau et al., "Ghosting comparison for large-area selenium detectors suitable for mammography and general radiography," *Proc. SPIE* **5368**, 162–169 (2004).

58. D. Hoeschen, "DQE of digital x-ray imaging systems: a challenge for standardization," *Proc. SPIE* **4320**, 280–286 (2001).

59. A. D. A. Maidment et al., "Standardization of NPS measurement: interim report of AAPM TG16," *Proc. SPIE* **5030**, 5230532 (2003).

60. J. H. Siewerdsen and L. E. Antonuk, "DQE and system optimization for indirect-detection flat-panel imagers in diagnostic radiology," *Proc. SPIE* **3336**, 546 (1998).

61. I. A. Cunningham, J. Yao, and V. Subotic, "Cascaded models and the DQE of flat-panel imagers: noise aliasing, secondary quantum noise, and reabsorption," *Proc. SPIE* **4682**, pp. 61–72 (2002).

62. K. S. Karim, A. Nathan, and J. A. Rowlands, "Alternate pixel architectures for large-area medical imaging," *Proc. SPIE* **4320**, 35–46 (2001).

63. L. E. Antonuk et al., "Exploration of the potential performance of polycrystalline silicon-based active matrix flat-panel imagers incorporating active pixel sensor architectures," *Proc. SPIE* **6913**, 69130I (2008).

64. M. P. Andre et al., "Integrated CMOS-selenium x-ray detector for digital mammography," *Proc. SPIE* **3336**, 204–209 (1998).

65. T. Graeve and G. P. Weckler, "High-resolution CMOS imaging detector," *Proc. SPIE* **4320**, 68 (2001).

66. D. Scheffer, "A wafer scale active pixel CMOS image sensor for generic x-ray radiology," *Proc. SPIE* **6510**, 65100O (2007).

67. S. K. Heo et al., "12-inch-wafer-scale CMOS active-pixel sensor for digital mammography," *Proc. SPIE* **7961**, 79610O (2011).

68. W. H. Maes et al., "Low-dose performance of wafer-scale CMOS-based x-ray detectors," *Proc. SPIE* **9412**, 94120C (2015).

69. A. Ganguly et al., "X-ray performance of new high dynamic range CMOS detector," *Proc. SPIE* **10573**, 105730N (2018).

70. W. H. Maes et al., "Extended dynamic range CMOS active pixel architecture for x-ray detectors," *Proc. SPIE* **11312**, 113123Z (2020).

71. D. L. Y. Lee, "Selenium detector with a grid for selenium charge gain," *Proc. SPIE* **5745**, 216 (2005).

72. J. R. Scheuermann et al., "Solid-state flat panel imager with avalanche amorphous selenium," *Proc. SPIE* **9783**, 978317 (2016).

73. W. Zhao et al., "Indirect flat-panel detector with avalanche gain: design and operation of the avalanche photoconductor," *Proc. SPIE* **5745**, 352 (2005).

74. S. Adachi et al., "Experimental evaluation of a-Se and CdTe flat-panel x-ray detectors for digital radiography and fluoroscopy," *Proc. SPIE* **3977**, 38 (2000).

75. R. A. Street et al., "High-resolution direct-detection x-ray imagers," *Proc. SPIE* **3977**, 418 (2000).

76. M. Simon et al., "PbO as direct conversion x-ray detector material," *Proc. SPIE* **5368**, 188–199 (2004).

77. G. Zentai et al., "Mercuric iodide medical imagers for low-exposure radiography and fluoroscopy," *Proc. SPIE* **5368**, 200–210 (2004).
78. U. Lemmer and H. Mescher, "Novel hybrid organic-inorganic perovskite detector designs based on multilayered device architectures: simulation and design," *Proc. SPIE* **10948**, 109480W (2019).
79. S. Shapiro, P. Strax, and L. Venet, "Periodic breast cancer screening in reducing mortality from breast cancer," *J. Am. Med. Assoc.* **215**(11), 1777 (1971).
80. C. Coleman, "Early detection and screening for breast cancer," *Semin. Oncol. Nurs.* **33**(2), 141–155 (2017).
81. M. J. Yaffe, J. G. Mainprize, and R. A. Jong, "Technical developments in mammography," *Health Phys.* **95**(5), 599–611 (2008).
82. A. G. Haus, "Screen-film mammography update: x-ray units, breast compression, grids, screen-film characteristics, and radiation dose," *Proc. SPIE* **0486**, 152 (1984).
83. A. D. A. Maidment et al., "Imaging performance of a prototype scanned-slot digital mammography system," *Proc. SPIE* **1896**, 93–103 (1993).
84. J. G. Yorker et al., "Characterization of a full-field digital mammography detector based on direct x-ray conversion in selenium," *Proc. SPIE* **4682**, 21–29 (2002).
85. D. Albagli et al., "Performance of advanced a-Si/CsI-based flat-panel x-ray detectors for mammography," *Proc. SPIE* **5030**, 553–563 (2003).
86. K. Irisawa et al., "Direct-conversion 50 $\mu$m pixel-pitch detector for digital mammography using amorphous selenium as a photoconductive switching layer for signal charge read-out," *Proc. SPIE* **7258**, 72581I (2009).
87. M. Danielsson et al., "Dose-efficient system for digital mammography," *Proc. SPIE* **3977**, 239–249 (2000).
88. S. J. Thunberg et al., "Evaluation of a photon-counting mammography system," *Proc. SPIE* **4682**, 202–208 (2002).
89. B. Ghammraoui, S. Gkoumas, and S. J. Glick, "Characterization of a GaAs photon-counting detector for mammography," *J. Med. Imaging* **8**(03), 33504 (2021).
90. J. Law, "The development of mammography," *Phys. Med. Biol.* **51**(13), R155–R167 (2006).
91. A. Fieselmann et al., "Full-field digital mammography with grid-less acquisition and software-based scatter correction: investigation of dose saving and image quality," *Proc. SPIE* **8668**, 86685Y (2013).
92. J. M. Lewin et al., "Dual-energy contrast-enhanced digital subtraction mammography: feasibility," *Radiology* **229**(1), 261–268 (2003).
93. R. A. Jong et al., "Contrast-enhanced digital mammography: initial clinical experience," *Radiology* **228**(3), 842–850 (2003).
94. T. Wu et al., "Digital tomosynthesis mammography using a parallel maximum-likelihood reconstruction method," *Proc. SPIE* **5368**, 1–11 (2004).
95. M. Bissonnette et al., "Digital breast tomosynthesis using an amorphous selenium flat panel detector," *Proc. SPIE* **5745**, 529 (2005).
96. B. Ren et al., "Design and performance of the prototype full field breast tomosynthesis system with selenium based flat panel detector," *Proc. SPIE* **5745**, 550–561 (2005).
97. J. W. Eberhard et al., "High-speed large-angle mammography tomosynthesis system," *Proc. SPIE* **6142**, 61420C (2006).
98. A.-K. Carton et al., "Dual-energy subtraction for contrast-enhanced digital breast tomosynthesis," *Proc. SPIE* **6510**, 651007 (2007).
99. S. Puong et al., "Dual-energy contrast enhanced digital breast tomosynthesis: concept, method, and evaluation on phantoms," *Proc. SPIE* **6510**, 65100U (2007).
100. S. J. Glick, "Breast CT," *Annu. Rev. Biomed. Eng.* **9**(1), 501–526 (2007).
101. J. M. Boone et al., "Performance assessment of a pendant-geometry CT scanner for breast cancer detection," *Proc. SPIE* **5745**, 319 (2005).
102. M. Dustler et al., "Can mechanical imaging increase the specificity of mammography screening?" *Eur. Radiol.* **27**(8), 3217–3225 (2017).
103. D. Förnvik et al., "Pressure distribution in mammography: compression of breasts with malignant tumor masses," *Proc. SPIE* **8668**, 86684E (2013).

104. C. A. Mistretta, "Real-time digital x-ray subtraction imaging," US Patent 4,204,225 (1980).
105. C. A. Mistretta, R. A. Kruger, and T. L. Houk, "Real-time digital x-ray time interval difference imaging," US Patent 4,204,226 (1980).
106. C. H. Slump, "Restoration of noise aliasing and Moire distortion in CCD-based diagnostic x-ray imaging," *Proc. SPIE* **1652**, 451–462 (1992).
107. M. Overdick, T. Solf, and H.-A. Wischmann, "Temporal artifacts in flat dynamic x-ray detectors," *Proc. SPIE* **4320**, 47–58 (2001).
108. M. Prümmer et al., "Multi-modal 2D-3D non-rigid registration," *Proc. SPIE* **6144**, 61440X (2006).
109. Y. Jiang and E. Ekanayake, "Stent enhancement using a locally adaptive unsharp masking filter in digital x-ray fluoroscopy," *Proc. SPIE* **9034**, 90342G (2014).
110. E. C. Lasser, N. A. Baily, and R. L. Crepeau, "A fluoroplanigraphy system for rapid presentation of single plane body sections," *Am. J. Roentgenol.* **113**(3), 574–577 (1971).
111. N. A. Baily and T. D. Kampp, "Digitized longitudinal tomography system," *Proc. SPIE* **0314**, 37–41 (1981).
112. R. J. Warp, D. J. Godfrey, and J. T. Dobbins III, "Applications of matrix inversion tomosynthesis," *Proc. SPIE* **3977**, 376 (2000).
113. G. Lauritsch and W. H. Haerer, "Theoretical framework for filtered back projection in tomosynthesis," *Proc. SPIE* **3338**, 1127–1137 (1998).
114. T. Mertelmeier et al., "Optimizing filtered backprojection reconstruction for a breast tomosynthesis prototype device," *Proc. SPIE* **6142**, 61420F (2006).
115. E. Y. Sidky et al., "Practical iterative image reconstruction in digital breast tomosynthesis by non-convex TpV optimization," *Proc. SPIE* **6913**, 691328 (2008).
116. M. J. Flynn, R. McGee, and J. Blechinger, "Spatial resolution of x-ray tomosynthesis in relation to computed tomography for coronal/sagittal images of the knee," *Proc. SPIE* **6510**, 65100D (2007).
117. T. Deller et al., "Effect of acquisition parameters on image quality in digital tomosynthesis," *Proc. SPIE* **6510**, 65101L (2007).
118. J. T. Dobbins et al., "Multi-institutional evaluation of digital tomosynthesis, dual-energy radiography, and conventional chest radiography for the detection and management of pulmonary nodules," *Radiology* **282**(1), 236–250 (2017).
119. C. R. Inscoe et al., "Stationary intraoral tomosynthesis for dental imaging," *Proc. SPIE* **10132**, 1013203 (2017).
120. T. Stalbaum et al., "200 kV x-ray source for radiotherapy and imaging: preliminary results and discussion," *Proc. SPIE* **11312**, 113123I (2020).
121. A. S. Chawla et al., "Optimized acquisition scheme for multi-projection correlation imaging of breast cancer," *Proc. SPIE* **6915**, 691528 (2008).
122. C. Zhao et al., "Third generation anthropomorphic physical phantom for mammography and DBT: incorporating voxelized 3D printing and uniform chest wall QC region," *Proc. SPIE* **10132**, 101321Y (2017).
123. M. L. Nock et al., "Quantitative flow phantom for contrast-enhanced breast tomosynthesis," *Proc. SPIE* **6510**, 65102W (2007).
124. E. G. Solomon et al., "Scanning-beam digital x-ray (SBDX) system for cardiac angiography," *Proc. SPIE* **3659**, 246–257 (1999).
125. F. Sprenger et al., "Stationary digital breast tomosynthesis with distributed field emission x-ray tube," *Proc. SPIE* **7961**, 79615I (2011).
126. R. Ning et al., "Selenium flat-panel detector-based volume tomographic angiography imaging: phantom studies," *Proc. SPIE* **3336**, 316–324 (1998).
127. D. A. Jaffray, J. H. Siewerdsen, and D. G. Drake, "Performance of a volumetric CT scanner based upon a flat-panel imager," *Proc. SPIE* **3659**, 204–214 (1999).
128. J. H. Siewerdsen et al., "Flat-panel cone-beam CT: a novel imaging technology for image-guided procedures," *Proc. SPIE* **4319**, 435–444 (2001).
129. R. Fahrig and D. W. Holdsworth, "Three-dimensional computed tomographic reconstruction using a C-arm mounted XRII: image-based correction of gantry motion nonidealities," *Med. Phys.* **27**(1), 30–38 (2000).

130. R. Ning et al., "Flat-panel detector-based cone-beam volume CT breast imaging: preliminary phantom study," *Proc. SPIE* **4320**, 601–610 (2001).
131. A. Kwan et al., "Progress in the development of a dedicated breast CT scanner," *Proc. SPIE* **5368**, 304 (2004).
132. W. Zbijewski et al., "Design and optimization of a dedicated cone-beam CT system for musculoskeletal extremities imaging," *Proc. SPIE* **7961**, 796104 (2011).
133. J. H. Siewerdsen and D. A. Jaffray, "Cone-beam CT with a flat-panel imager: noise considerations for fully 3D computed tomography," *Proc. SPIE* **3977**, 408–416 (2000).
134. A. Malusek, M. P. Sandborg, and G. A. Carlsson, "Simulation of scatter in cone beam CT: effects on projection image quality," *Proc. SPIE* **5030**, 740–751 (2003).
135. L. Zhu, N. Strobel, and R. Fahrig, "X-ray scatter correction for cone-beam CT using moving blocker array," *Proc. SPIE* **5745**, 251 (2005).
136. A. Sisniega et al., "Image-based motion compensation for high-resolution extremities cone-beam CT," *Proc. SPIE* **9783**, 97830K (2016).
137. J. W. Stayman et al., "Model-based reconstruction of objects with inexactly known components," *Proc. SPIE* **8313**, 83131S (2012).
138. G. J. Gang et al., "Modeling and control of nonstationary noise characteristics in filtered-backprojection and penalized likelihood image reconstruction," *Proc. SPIE* **8668**, 86681G (2013).
139. S. Ouadah et al., "Task-driven orbit design and implementation on a robotic C-arm system for cone-beam CT," *Proc. SPIE* **10132**, 101320H (2017).
140. B. Nett et al., "Low radiation dose C-arm cone-beam CT based on prior image constrained compressed sensing (PICCS): including compensation for image volume mismatch between multiple data acquisitions," *Proc. SPIE* **7258**, 725803 (2009).
141. J. W. Stayman et al., "Penalized-likelihood reconstruction for sparse data acquisitions with unregistered prior images and compressed sensing penalties," *Proc. SPIE* **7961**(1), 79611L (2011).
142. Y. Li and G.-H. Chen, "Deep learning based cone beam CT reconstruction framework using a cascaded neural network architecture," *Proc. SPIE* **10573**, 105731J (2018).
143. D. L. Parker, "Optimization of short scan convolution reconstruction in fan beam CT," *Proc. SPIE* **0372**, 199–202 (1982).
144. C. R. Crawford and K. F. King, "Simultaneous patient translation during CT scanning," *Proc. SPIE* **1443**, 203–213 (1991).
145. P. J. La Riviere and X. Pan, "Fourier-based approach to interpolation in helical CT exploiting redundant fan-beam information," *Proc. SPIE* **3977**, 280–291 (2000).
146. G. M. Besson, "Multislice single-filtering helical-weighting algorithm," *Proc. SPIE* **3977**, 258–269 (2000).
147. J. Hsieh and X. Tang, "Conjugate backprojection approach for cone beam artifact reduction," *Proc. SPIE* **6142**, 614225 (2006).
148. X. Tang, J. Hsieh, and R. A. Nilsen, "3D-weighted cone beam filtered backprojection (CB-FBP) algorithm for image reconstruction at low-helical pitches to improve noise characteristics and dose efficiency," *Proc. SPIE* **6142**, 614227 (2006).
149. X. Tang and J. Hsieh, "Ray-wise weighted helical cone beam filtered backprojection algorithm for image reconstruction under moderate cone angle," *Proc. SPIE* **6510**, 65105O (2007).
150. E. Cesmeli et al., "Novel reconstruction algorithm for multiphasic cardiac imaging using multislice helical CT," *Proc. SPIE* **4320**, 645–654 (2001).
151. H. Bruder et al., "Flash imaging in dual source CT (DSCT)," *Proc. SPIE* **7258**, 72580D (2009).
152. A. Imiya and H. Ogawa, "Direct reconstruction of three dimensional image from its line integrals," *Proc. SPIE* **0671**, 42 (1986).
153. H. Hu, G. T. Gullberg, and R. A. Kruger, "A convolution backprojection reconstruction algorithm for use with an image intensifier detector," *Proc. SPIE* **0914**, 542 (1988).
154. S. W. Lee and G. Wang, "Grangeat-type half-scan algorithm for cone beam CT," *Proc. SPIE* **5030**, 980 (2003).
155. H. Hu, "New cone-beam reconstruction algorithm and its application to circular orbits," *Proc. SPIE* **2163**, 223–234 (1994).

156. Z. Dai et al., "Accelerating 3D cone beam T-FDK algorithm on commodity PC graphics hardware," *Proc. SPIE* **6142**, 61424P (2006).
157. F. Noo and D. J. Heuscher, "Image reconstruction from cone-beam data on a circular short-scan," *Proc. SPIE* **4684**, 50–59 (2002).
158. K. C. Tam, S. Samarasekera, and F. Sauer, "Region-of-interest cone-beam CT with a spiral scan," *Proc. SPIE* **3336**, 274 (1998).
159. M. King et al., "Chord-based image reconstruction from clinical projection data," *Proc. SPIE* **6913**, 69132G (2008).
160. H. Hu, "Exact regional reconstruction of longitudinally unbounded objects using the circle-and-line cone-beam tomographic system," *Proc. SPIE* **3032**, 441–444 (1997).
161. C. E. Yarman and B. Yazıcı, "An inversion method for the cone-beam transform," *Proc. SPIE* **6142**, 61424C (2006).
162. Z. Yin, B. De Man, and J. Pack, "Analytical cone-beam reconstruction using a multi-source inverse geometry CT system," *Proc. SPIE* **6510**, 651021 (2007).
163. A. A. Zamyatin et al., "Implementation of the circle-and-line algorithm for 256-detector row CT," *Proc. SPIE* **6510**, 65105D (2007).
164. Z. Yu et al., "Ellipse-line-ellipse source trajectory and its R-line coverage for long-object cone-beam imaging with a C-arm system," *Proc. SPIE* **8313**, 83133E (2012).
165. S. Schaller, T. Flohr, and P. Steffen, "New efficient Fourier-reconstruction method for approximate image reconstruction in spiral cone-beam CT at small cone angles," *Proc. SPIE* **3032**, 213–224 (1997).
166. W.-T. Lin, "Computationally efficient cone beam CT reconstruction algorithm using circle-and-line orbit," *Proc. SPIE* **3659**, 933–943 (1999).
167. J. Brokish, D. B. Keesing, and Y. Bresler, "Iterative circular conebeam CT reconstruction using fast hierarchical backprojection/reprojection operators," *Proc. SPIE* **7622**, 76221R (2010).
168. K. Schmitt et al., "FINESSE: a fast iterative non-linear exact sub-space SEarch based algorithm for CT imaging," *Proc. SPIE* **9033**, 90330Q (2014).
169. O. Bockenbach, M. Knaup, and M. Kachelrieß, "Implementation of a cone-beam back-projection algorithm on the cell broadband engine processor," *Proc. SPIE* **6510**, 651056 (2007).
170. J. Nebeker, T. R. Nelson, and J. M. Boone, "Fast arbitrary-slice CT reconstruction with GPUs," *Proc. SPIE* **6510**, 651059 (2007).
171. H. Zheng et al., "Investigation on PI-line selecting method base on GPU accelerated back-projection filtered VOI reconstruction," *Proc. SPIE* **7622**, 76222G (2010).
172. L. Xie et al., "A rapid parallelization of cone-beam projection and back-projection operator based on texture fetching interpolation," *Proc. SPIE* **9412**, 94122S (2015).
173. D. Schlifske and H. Medeiros, "A fast GPU-based approach to branchless distance-driven projection and back-projection in cone beam CT," *Proc. SPIE* **9783**, 97832W (2016).
174. J. Min et al., "Low-dose dual-energy cone-beam CT using a total-variation minimization algorithm," *Proc. SPIE* **7961**, 796132 (2011).
175. S. Rose, E. Y. Sidky, and X. Pan, "Application of a non-convex smooth hard threshold regularizer to sparse-view CT image reconstruction," *Proc. SPIE* **9412**, 941206 (2015).
176. Y. Tang and C. Zong, "A new approach to solving the prior image constrained compressed sensing (PICCS) with applications in CT image reconstruction," *Proc. SPIE* **10132**, 101322T (2017).
177. C. Zhang, Y. Li, and G. Chen, "Deep learning enabled prior image constrained compressed sensing (DL-PICCS) reconstruction framework for sparse-view reconstruction," *Proc. SPIE* **11312**, 1131206 (2020).
178. H. Gong et al., "Ultra-fast-pitch acquisition and reconstruction in helical CT," *Proc. SPIE* **11312**, 1131209 (2020).
179. J. Llacer, S. Andreae, and A. Chatterjee, "On the applicability of the maximum likelihood estimator algorithm for image recovery in accelerated positron emitter beam injection," *Proc. SPIE* **0671**, 269 (1986).
180. J. Llacer et al., "On the convergence of the maximum likelihood estimator method of tomographic image reconstruction," *Proc. SPIE* **0767**, 70–76 (1987).

181. C. E. Metz and C.-T. Chen, "On the acceleration of maximum likelihood algorithms," *Proc. SPIE* **0914**, 344 (1988).

182. E. Y. Sidky et al., "Prototyping optimization problems for digital breast tomosynthesis image reconstruction with a primal-dual algorithm," *Proc. SPIE* **10948**, 1094852 (2019).

183. M. Gao et al., "Deep convolutional neural network denoising for digital breast tomosynthesis reconstruction," *Proc. SPIE* **11312**, 113120Q (2020).

184. W. A. Kalender et al., "Spiral volumetric CT with single-breath-hold technique, continuous transport, and continuous scanner rotation," *Radiology* **176**(1), 181–183 (1990).

185. C. R. Crawford and K. F. King, "Computed tomography scanning with simultaneous patient translation," *Med. Phys.* **17**(6), 967–982 (1990).

186. C. H. McCollough and F. E. Zink, "Performance evaluation of a multi-slice CT system," *Med. Phys.* **26**(11), 2223–2230 (1999).

187. K. Klingenbeck-Regn et al., "Subsecond multi-slice computed tomography: basics and applications," *Eur. J. Radiol.* **31**(2), 110–124 (1999).

188. B. Ohnesorge et al., "Cardiac imaging by means of electrocardiographically gated multi-section spiral CT: initial experience," *Radiology* **217**(2), 564–571 (2000).

189. J. Hsieh, "Two-pass algorithm for cone-beam reconstruction," *Proc. SPIE* **3979**, 533–540 (2000).

190. M. D. Silver et al., "Windmill artifact in multislice helical CT," *Proc. SPIE* **5032**, 1918 (2003).

191. H. Bruder et al., "Adaptive iterative reconstruction," *Proc. SPIE* **7961**, 79610J (2011).

192. B. De Man et al., "Multi-source inverse geometry CT: a new system concept for x-ray computed tomography," *Proc. SPIE* **6510**, 65100H (2007).

193. J. A. Fessler et al., "Maximum-likelihood dual-energy tomographic image reconstruction," *Proc. SPIE* **4684**, 38–49 (2002).

194. Y. Zou and M. D. Silver, "Analysis of fast kV-switching in dual energy CT using a pre-reconstruction decomposition technique," *Proc. SPIE* **6913**, 691313 (2008).

195. C. Eusemann et al., "Dual energy CT: how to best blend both energies in one fused image?" *Proc. SPIE* **6918**, 691803 (2008).

196. X. Wu et al., "Monochromatic CT image representation via fast switching dual kVp," *Proc. SPIE* **7258**, 725845 (2009).

197. P. R. S. Mendonça et al., "Multi-material decomposition of spectral CT images," *Proc. SPIE* **7622**, 76221W (2010).

198. X. Liu et al., "Quantitative imaging of chemical composition using dual-energy, dual-source CT," *Proc. SPIE* **6913**, 69134Z (2008).

199. K. Rajendran et al., "High resolution, full field of view, whole body photon-counting detector CT: system assessment and initial experience," *Proc. SPIE* **11595**, 115950D (2021).

200. W. C. Barber et al., "Characterization of a novel photon counting detector for clinical CT: count rate, energy resolution, and noise performance," *Proc. SPIE* **7258**, 725824 (2009).

201. S. Kappler et al., "First results from a hybrid prototype CT scanner for exploring benefits of quantum-counting in clinical CT," *Proc. SPIE* **8313**, 83130X (2012).

202. S. Kappler et al., "Photon counting CT at elevated x-ray tube currents: contrast stability, image noise and multi-energy performance," *Proc. SPIE* **9033**, 90331C (2014).

203. L. Gjesteby et al., "Deep learning methods to guide CT image reconstruction and reduce metal artifacts," *Proc. SPIE* **10132**, 101322W (2017).

204. D. P. Clark, M. Holbrook, and C. T. Badea, "Multi-energy CT decomposition using convolutional neural networks," *Proc. SPIE* **10573**, 105731O (2018).

205. R. Steadman et al., "ChromAIX: a high-rate energy-resolving photon-counting ASIC for spectal computed tomography," *Proc. SPIE* **7622**, 762220 (2010).

206. A. Zang et al., "Characterization of a hybrid energy-resolving photon-counting detector," *Proc. SPIE* **9033**, 90333M (2014).

207. M. Persson et al., "Energy-resolved CT imaging with a photon-counting silicon-strip detector," *Phys. Med. Biol.* **59**(22), 6709–6727 (2014).

208. A. S. Wang and N. J. Pelc, "Impact of photon counting detector spectral response on dual energy techniques," *Proc. SPIE* **7622**, 76223L (2010).

209. J. Cammin et al., "Compensation of nonlinear distortions in photon-counting spectral CT: deadtime loss, spectral response, and beam hardening effects," *Proc. SPIE* **8313**, 83131T (2012).

210. S. S. Hsieh and N. J. Pelc, "Pulse detection logic for multibin photon counting detectors: beyond the simple comparator," *Proc. SPIE* **9412**, 941210 (2015).

211. J. Dickmann et al., "A count rate-dependent method for spectral distortion correction in photon counting CT," *Proc. SPIE* **10573**, 1057311 (2018).

212. Y. Yang, N. Pelc, and A. Wang, "Analytical model for pulse pileup in photon counting detectors with seminonparalyzable behavior," *Proc. SPIE* **11595**, 115951Z (2021).

213. F. Rupcich and T. Gilat-Schmidt, "Experimental study of optimal energy weighting in energy-resolved CT using a CZT detector," *Proc. SPIE* **8668**, 86681X (2013).

214. C. Schirra et al., "Towards in-vivo K-edge imaging using a new semi-analytical calibration method," *Proc. SPIE* **9033**, 90330N (2014).

215. J. Rajagopal et al., "Impact of energy threshold on material quantification of contrast agents in photon-counting CT," *Proc. SPIE* **10948**, 109484N (2019).

216. A. P. Harrison, S. Ulzheimer, and A. Pourmorteza, "Maximum a posteriori material decomposition for spectral photon-counting CT: application to human blood iron level estimation," *Proc. SPIE* **11595**, 115954H (2021).

217. D. Muenzel et al., "Photon counting CT of the liver with dual-contrast enhancement," **Proc. 9783**, 97835N (2016).

218. R. Gutjahr et al., "Dual energy CT kidney stone differentiation in photon counting computed tomography," *Proc. SPIE* **10132**, 1013237 (2017).

219. A. Viry et al., "Multi-energy spectral photon-counting CT in crystal-related arthropathies: initial experience and diagnostic performance in vitro," *Proc. SPIE* **10573**, 1057351 (2018).

220. F. Grönberg et al., "Feasibility of unconstrained three-material decomposition: imaging an excised human heart using a prototype silicon photon-counting CT detector," *Eur. Radiol.* **30**(11), 5904–5912 (2020).

221. M. Danielsson, M. Persson, and M. Sjölin, "Photon-counting x-ray detectors for CT," *Phys. Med. Biol.* **66**(3), 03TR01 (2021).

222. C. Sundberg et al., "1 $\mu$m spatial resolution in silicon photon-counting CT detectors by measuring charge diffusion," *Proc. SPIE* **11312**, 113120E (2020).

223. X. Ji et al., "Phase contrast CT enabled three-material decomposition in spectral CT imaging," *Proc. SPIE* **11312**, 113121B (2020).

**Adam Wang** is an assistant professor in the Department of Radiology at Stanford University. He received his BS degree in electrical engineering from the University of Texas at Austin and his PhD in electrical engineering from Stanford University. He is the author of more than 60 journal papers. His research interests include dual-energy x-ray imaging, photon-counting CT, and optimizing CT dose and noise.

**Ian Cunningham** is a research scientist at the Robarts Research Institute and professor at Western University in the Department of Medical Biophysics with appointments in biomedical engineering and medical imaging. His research interests include the application of physics and engineering to the development of image science and new medical-imaging instrumentation and methods. He has published more than 175 articles on topics including coherent-scatter computed tomography, digital radiography, dual-energy imaging, development of cascaded-systems theory, and photon-counting technologies.

**Mats Danielsson** is a professor at KTH Royal Institute of Technology and division leader in physics of medical imaging as well as program leader at MedTechLabs at KTH and the Karolinska Hospital, Stockholm. He received his PhD in physics for research conducted at Conseil Européen pour la Recherche Nucléaire and was a postdoc at Lawrence Berkeley National Laboratory. His main research interests are photon-counting detectors and x-ray optics and he has 120 publications in the *Journal of Medical Imaging*, *Medical Physics*, PMB, *Nature*, and other respected journals. He also holds more than 100 patents and based on the research cofounded Sectra Mamea AB (acquired by Philips), C-RAD AB (listed on Nasdaq), and Prismatic Sensors (acquired by GE Healthcare).

**Rebecca Fahrig** is head of innovation for the business area advanced therapies at Siemens Healthcare GmbH, and professor in the Department of Computer Science at the Pattern Recognition Lab at Friedrich–Alexander Universitat, Erlangen, Germany. She received her BSc degree in physics and his MSc degree in medical biophysics from the University of Toronto, and his PhD in medical biophysics from the University of Western Ontario in London, Ontario, Canada. Her research and predevelopment work focus on multimodality image guidance technologies for use during planning, guidance, and assessment of minimally invasive therapies. She is a fellow of the AAPM and AIMBE.

**Thomas Flohr** received his PhD in physics from Erlangen University, Erlangen, Germany. He joined Siemens Healthcare in 1989 and was instrumental in developing multidetector row CT, cardiac CT, dual-source CT, and photon-counting CT. In 2002, he was the finalist (together with Bernd Ohnesorge) for the "Innovation Prize of the German President" for his work on cardiac CT. He is an adjunct professor of medical physics at Tübingen University, Tübingen, Germany. He holds more than 100 patents and is an author and a coauthor of more than 200 peer-reviewed publications.

**Frederic Noo** received his PhD in engineering sciences from the University of Liege, Belgium in 1998, on the topic of image reconstruction methods for cone-beam tomography. He is a tenured professor at the University of Utah where he relocated in 2001, with research interests covering all physics and mathematical aspects of image reconstruction and image quality assessment for computed tomography.

**John M. Sabol** received his PhD in medical biophysics from the University of Toronto in 1996. He has worked for three major medical imaging companies as a scientist and researcher. While Chief Scientist at GE Healthcare he did research across many systems and modalities including the development and clinical validation of dual-energy and tomosynthesis applications of digital radiography. Currently, he is doing similar research at Konica Minolta Healthcare with a focus on the development and expansion of dynamic digital radiography applications.

**Jeffrey H. Siewerdsen** received his PhD in physics from the University of Michigan in 1998, where he worked on the early development of flat-panel x-ray detectors. At William Beaumont Hospital (Royal Oak, Michigan), he was on the team that developed the first systems for cone-beam CT image-guided radiation therapy. At the University of Toronto and Ontario Cancer Institute/Princess Margaret Hospital (Toronto, Ontario), his research expanded to the development of mobile intraoperative cone-beam CT systems for image-guided surgery. Currently, he is John C. Malone Professor and Vice-Chair in the Department of Biomedical Engineering at Johns Hopkins University (Baltimore, Maryland), where he leads a research program for image-guided interventions and codirects the Carnegie Center for Surgical Innovation.

**Anders Tingberg**, PhD, is an associate professor, a certified medical physicist, and head of the department for x-ray and MRI physics at Skåne University Hospital, and affiliated to Lund University. He has authored or coauthored more than 100 peer-reviewed or conference papers. His main research focus interest is in breast imaging, especially breast tomosynthesis.

**Wei Zhao** received her PhD in medical physics from the University of Toronto. She is a professor of radiology and biomedical engineering at Stony Brook University. Her main research interest is in the development and clinical translation of medical imaging detector technologies

**Ehsan Samei**, PhD, DABR, FAAPM, FSPIE, FAIMBE, FIOMP, FACR, is a tenured professor and chief imaging physicist at Duke University Health System. He has authored more than 300 referred papers. He is passionate about bridging the gap between scientific scholarship and clinical practice through virtual clinical trials and clinically-relevant imaging metrics, such that they could enable optimum quantitative use of imaging, a realization of translational research, and clinical processes that are based on evidence.

Biographies of the other authors are not available.